Predictive models building to assess the state of deterioration in the availability of nutrients (N, P and K) in the soil with time by remote sensing data

Abdulsalam Mashaal Faisal Aljumaily[1]
[1]University of Mosul, College of Agriculture and Forestry, Department of Soil Sciences and Water Resources. Iraq. abdulsalam.faisal@uomosul.edu.iq

Dr. Ammar Younes Ahmed Kashmoola[2]
[2]University of Mosul, College of Agriculture and Forestry, Department of Soil Sciences and Water Resources. Iraq. ammaryajk60@uomosul.edu.iq

Corresponding author : Abdulsalam Mashaal Faisal Aljumaily

Abstract

Agricultural fields close to Rabia district, northwest of Nineveh Governorate / Iraq were selected for the study, as the study area is located between the points (36°31'51.34'' and 36°43'40.343'') north and the points (24°16'14.475'' and 42° 34'50.99'') east, and the study area was approximately 52.5 hectares (210) km2. Predictive models were built resulting from multiple linear and nonlinear regression relationships between remote sensing data and ready concentration values of the three necessary components (N, P and K) measured in the laboratory, in order to apply the predictive model to space data for previous years and assess the state of deterioration in soil fertility for two decades of time.

The results of the study showed the possibility of applying predictive models to space data for previous years to give results with a high spatial accuracy of (0.9713, 0.9492 and 0.9670) for nitrogen, phosphorous and potassium, respectively. Spatial maps could be drawn for each of the three studied years (2002, 2012 and 2022) and for each of the three studied nutrients. The amount of deterioration that occurred and a decrease in the concentration of nutrients over time was observed as a result of bad management and poor exploitation of the earth's resources.

Key words: nitrogen, phosphorous, potassium, soil fertility, remote sensing, predictive models.

Conflict of Interest : There is no conflict of interest

DOI Number: 10.14704/nq.2022.20.9.NQ44799 **Neuro Quantology 2022; 20(9):6839-6847**

Introduction

The distribution of nutrients necessary for plant life and the different values of fertility standards from one agricultural field to another are among the details entrusted to those responsible for managing and maintaining soil fertility to know and care about it. The diagnosis and estimation of the amount of organic matter, the degree of reaction, the salt concentration and the necessary ready-made elements are among the fertility tests necessary to assess the productivity of agricultural land, and through the difference and variance that we obtain compared to previous years, it is possible to assess the amount of deterioration in soil fertility (Adamu et al., 2014). As a result of the speed at which soil fertility is subject to deterioration, it has become necessary to study the deterioration using space data to diagnose the amount of deterioration in large areas and in the least possible time to prevent the danger of unjustified fertilizer additions and to maintain the environmental balance of the soil and its surroundings (Wu, 2011). The integration of remote sensing data with laboratory test values enabled Prudnikova et al. (2021) to build predictive models that enable them to prepare digital maps for some soil chemical properties. Also, the use of remote sensing data and its mathematical relationships with the digital values of laboratory tests of the chemical properties of the soil enabled Taha et.al (2014) to prepare digital maps for the

distribution of nitrate and ammonium concentrations in the soils of the northern parts of Babylon Governorate using the output of remote sensing data represented by spectral evidence (SAVI, OSAVI, GDVI).

Some characteristics of fertile soils can be predicted for successive prior years (Wu et al., 2014). And preparing digital maps by integrating laboratory tests with remote sensing data within predictive models, linear and non-linear regression formulas, and with spatial accuracy that surpasses traditional maps (Wu et al., 2014).

Materials and working methods

Experiment Site and Area

The agricultural fields near Rabi'a district, northwest of Nineveh Governorate / Iraq, were selected as an area to conduct the research, due to the lack of studies related to soil fertility using remote sensing that belong to this area and to suit the nature of the study, as the study area is located as measured by a GPS device between the two points. (36°31'51.34'' and 36°43'40.343'') N and the two points (24°16'14.475'' and 42°34'50.99'') E. The study area was 52.5 hectares (210) km2.

Soil sample collection

50 composite soil samples were taken, distributed almost uniformly over the studied area to be representative of the studied area. The samples were dried, then crushed and sieved with a sieve with a diameter of 2 mm and kept in polyethylene bags away from sunlight, then physical and chemical laboratory tests were conducted on them, the degree of reaction, the electrical conductivity of the soil solution, calcium carbonate, calcium sulfate, organic matter, ready-made nitrogen, Ready phosphorous, ready potassium, soluble calcium, soluble magnesium, soluble sodium, bicarbonate, chlorides (pH, EC, CaCO3, CaSO4, OM, N, P, K, Ca, Mg, Na, HCO3, Cl) respectively, and the methods were followed approved for it.

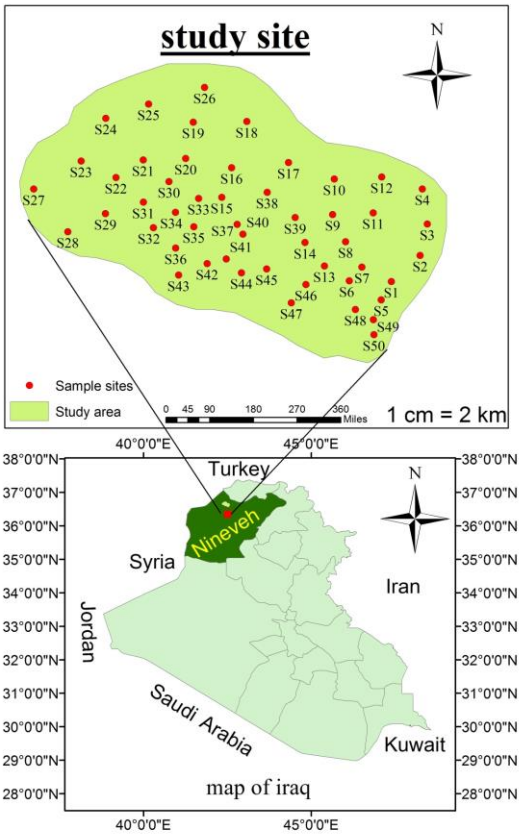

Figure (1): A map showing the study site.

A set of satellite data captured by the ETM+ (Enhanced Thematic Mapper plus) of the satellite (Landsat7) as well as by the combination of Land Imager and Thermal Infrared Sensors (OLI/TIRS C2 L1) (Operational Land Imager and Thermal Infrared) was used. Sensor Collection 2 Level-1) of the Landsat satellite (Landsat 8-9), and the Path and Row for this statement are (170 and 35) respectively. The three satellite images were taken on the dates (02/12/2002, 2/4/2012, and 2/7/2022).

Using the ENVI 5.3 program, satellite images were processed within the FLAASH (Fast Line of sight Atmospheric Analysis of Spectral Hypercube model) model to remove atmospheric effects and deduct the study area from the aerial image (Wu, 2011). The exponential and logarithmic values of the spectral indices were calculated to test the relationship of the spectral indices values with the laboratory-measured fertility concentrations of the study samples. As a result, the following spectral indices were selected:

1- NDVI (Normalized Differences Vegetation Index (Rouse and others, 1973).

NDVI = (NIR-RED)/(NIR+RED) ..... (1)

2- Enhanced Vegetation Index (EVI) (Huete et al., 1997).

EVI = 2.5 ((NIR-Red)/(NIR+ Red-7.5 Blue+1) ..(2)

3- Optimized Soil-Adjusted Vegetation Index (OSAVI) (Rondeaux, 1996).

OSAVI = (NIR-Red / (NIR+ Red+0.16) … (3)

4- Clay Index (Storey et al., 2014).

CL = (SWIR1/SWIR2) …….. (4)

5- The Visible Atmospherically Resistant Index (VARI) (Gitelson A., 2002).

VARI = (Green–Red) / (Green + Red–Blue)... (5)

6- Generalized Difference Vegetation Index (GDVI) Rouse et al., (1973).

GDVI2 = [(B4)2 - (B3)2] / [(B4)2 + (B3)2]… (6)

7- Salinity Index (SI) (Abbas and Khan, 2007).

SI = Green2 + Red2 + NIR2 ……. (7)

He used the (SPSS) and (Excel) program to calculate the value of the coefficient of determination R2 to find the statistical relationships between some variables, in addition to organizing tables, performing mathematical calculations, and preparing columns to clarify the differences between the study sites.

After finding the values of evidence that were affected by the reflexivity of the studied traits, which were extracted using the ArcGIS 10.8 program, then a correlation analysis and regression analysis were conducted. A predictive model equation to be applied to satellite visualizations for the years 2002, 2012 and 2022 in order to represent the fertility status of those years on color maps using Kriging and Reclassify technology in ArcGIS.

After the spectral indices values were extracted at each sample location from the samples taken, using the ENVI 5.3 program, these values were arranged in special tables corresponding to the names and numbers of the samples taken at them, then the exponential, linear and logarithmic relationships of these values were tested with the concentrations of the studied traits and the correlation relationship was studied Between the concentrations of each fertility trait on the one hand and the values of spectral indices and the values of the exponential, linear and logarithmic relationships using the SPSS statistical analysis program, which resulted in more than one predictive model and each model has a different degree of accuracy value (R2), the most accurate predictive models were selected based on the value of (R2). . The following predictive models were selected:

N = - 464.540 + 470.426 * Exp(OSAVI) - 35.462 * (GDVI) - 0.128 * (VARI) + 116.178 * (SI)…….. (R2 = 0.9713) ……. (8)

P = - 191.197 - 71.587 * (NDVI) + 20.287 * Exp(EVI) + 95.503 * Exp(OSAVI) … ……(R2 = 0.9492) ……..……(9)

K = - 1609.94 + 4.7 * (VARI) + 601.01 * Exp(CL) + 221.727 * (GDVI) ……. (R2 = 0.9670) ……..…….. (10)

After we obtained the predictive models above, their values were calculated, and the results were very close to the concentrations of fertility traits measured in the laboratory, through which they were relied upon in mapping nutrients for the three years studied using the ENVI 5.3 program, and then the resulting images were processed using the Arcmap 10.8 program to distinguish them. In color and perform the process of Reclassify and extract it with the percentage values of the limits of the concentrations of nutrients that have been studied.

The traits were represented within varieties at the limits and ranges of their concentration and content of each of them in the soil as shown in Table (1).

Table (1): Types of the studied traits and their ranges

Adjective	Categories			measruing unit
	Low	Medium	High	
ready-made nitrog	less than 30	30-50	greater than 50	**ppm**
ready-made phosphorous	less than 10	10-18	over 18	**ppm**
ready-made potassium	less than 160	160-250	greater than 250	**ppm**

Table (2): The physical and chemical properties measured in the laboratory

Site	texture	Av.N ppm	Av.P ppm	Av.K ppm	CEC mq/100g	O.M. %	$CaSO_3$ %	$CaCO_3$ %	EC dS/m	pH
1	SL	34.6	10.91	137.3	35.90	2.75	2.20	33	4.68	**7.2**
2	C	36.37	10.14	148.07	34.28	1.89	2.71	33.5	3.22	**7.2**
3	SL	32.47	12.83	157.50	43.78	2.92	1.98	26.5	4.97	7.3
4	CL	32.36	11.42	142.44	40.43	2.24	1.89	32.5	2.92	7.3
5	CL	35.88	10.04	134.45	39.34	1.65	2.46	23.5	3.04	7.3
6	CL	36.55	11.36	107.81	41.41	1.20	2.25	26	2.34	7.2
7	CL	33.23	13.52	197.84	38.05	2.06	2.42	22.5	1.46	7.3
8	SCL	35.47	10.58	111.79	39.05	1.03	2.17	26	2.92	7.3
9	SC	31.95	11.41	123.53	39.76	2.58	1.50	10	3.39	7.2
10	SCL	34.3	9.74	52.55	30.81	1.89	1.25	11	4.39	7.2
11	SCL	30.12	16.19	249.41	32.59	2.41	2.42	19	4.09	7.2
12	SCL	34.54	11.52	170.13	27.52	2.75	2.42	15	3.22	7.3
13	L	33.35	12.73	173.92	37.41	1.72	2.20	22	5.38	7.3
14	L	32.66	10.82	113.79	39.07	1.79	1.62	25.5	4.39	7.3
15	L	32.44	10.87	143.16	40.04	1.38	1.91	23.5	3.51	7.3
16	L	36.93	10.13	123.51	44.00	0.86	2.60	25	2.92	7.3
17	L	37.72	10.01	91.88	36.84	1.72	2.38	25	2.63	7.3
18	L	35.64	10.15	160.85	42.88	1.99	2.73	21.5	3.63	7.3
19	CL	32.51	12.29	142.17	35.95	2.58	1.90	21	3.39	7.2
20	SL	33.17	9.99	92.54	35.37	2.41	0.12	22	2.92	7.2
21	L	36.62	10.48	107.22	28.99	1.89	2.37	20.5	2.34	7.4
22	L	35.07	9.52	14.50	36.85	3.16	0.95	21	2.81	7.3
23	L	36.9	9.68	93.55	34.90	2.58	2.25	22.5	3.8	7.4
24	L	32.17	12.6	211.33	37.45	2.06	2.54	22	4.68	7.4
25	L	29.07	14.72	233.9	40.78	1.72	2.04	11.5	1.17	7.4
26	L	31.36	13.93	201.61	29.23	1.55	2.15	17.5	2.92	7.3
27	L	33.68	9.98	77.64	45.40	2.13	1.45	19.5	2.34	7.3
28	L	35.23	9.73	121.70	46.76	1.99	2.25	15.5	3.22	7.3
29	SCL	34.35	9.29	97.71	37.01	1.72	1.84	19.5	4.09	7.2
30	SCL	35.76	10.78	173.49	36.20	1.38	2.82	19	3.63	7.2
31	SCL	35.62	10.72	137.22	39.90	1.65	2.44	19.5	4.97	7.2
32	SCL	35.22	11.36	113.26	40.42	2.24	2.10	22	4.68	7.2
33	SCL	19.69	10.72	818.99	48.88	2.75	2.95	23	2.81	7.3
34	SL	35.19	10.5	145.75	33.91	0.69	2.46	20	3.22	7.2
35	SCL	36.26	10.25	130.49	39.94	1.72	2.42	18	4.68	7.2
36	SCL	35.42	11.14	131.48	42.52	1.38	2.37	18.5	2.92	7.3
37	SCL	34.44	10.44	132.12	35.94	1.89	2.21	21.5	4.79	7.2
38	SCL	29.2	18.77	255.89	45.99	2.41	2.24	14.5	3.51	7.2

39	SCL	33.54	10.23	151.85	36.23	2.13	2.19	27.5	2.63	7.4
40	SCL	32.52	11.14	226.18	41.59	2.92	2.45	21	2.92	7.2
41	SCL	32.81	11.37	142.47	43.54	2.75	1.94	15.5	3.63	7.2
42	L	35.54	9.89	100.99	40.90	1.65	2.15	31.5	3.8	7.3
43	SCL	32.65	12	173.38	38.22	1.89	2.11	17	2.81	7.2
44	SCL	33.82	9.96	116.89	35.23	2.75	1.84	13.5	2.05	7.3
45	SL	35.1	10.06	133.23	48.75	1.72	2.30	15.5	3.51	7.2
46	L	36.61	10.55	117.11	36.85	2.82	2.40	11.5	1.75	7.3
47	SCL	35.52	10.31	174.77	31.41	2.06	2.65	18	4.39	7.2
48	SCL	34.25	10.12	174.64	42.67	1.55	2.42	18.5	3.22	7.3
49	SL	35.6	10.33	132.77	37.53	1.72	2.39	25.5	4.09	7.3
50	L	36.59	10.95	158.57	35.37	2.13	2.87	19	4.68	7.3

Results and discussion

Nitrogen

The results in Figure (2) show that using the predictive model (Equation 8) gave good results in diagnosing the amount of ready nitrogen in the soil, with an accuracy of (R2 = 0.9713), and this is consistent with what was reached by Vagan et al. (2016), where They emphasized that it is possible to rely on remote sensing data and its outputs to estimate the amount of ready nitrogen in the soil, and this contributes to preparing high-accuracy spatial maps for adoption as a basic reference for agricultural workers and researchers in soil fertility survey as well as in estimating fertilizer needs and assessing the state of deterioration. The application of the predictive model of ready-made nitrogen (Equation 8) to the remote sensing data for the years 2002 and 2012 showed the amount of ready-made nitrogen in these two years, and this helped in monitoring the amount of deterioration that occurred by comparing these results with the results of the values of ready-made nitrogen in 2022, and for the three types (High and Medium and Low), as the deterioration in the amount of ready nitrogen between 2002 and 2012 and 2012 and 2022 was clear.

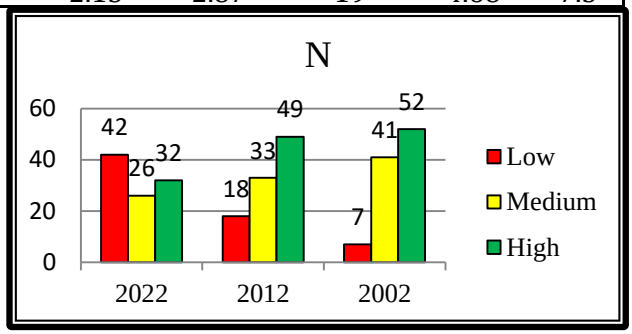

Figure (2): Percentages of the area of nitrogen values for varieties in the years studied.

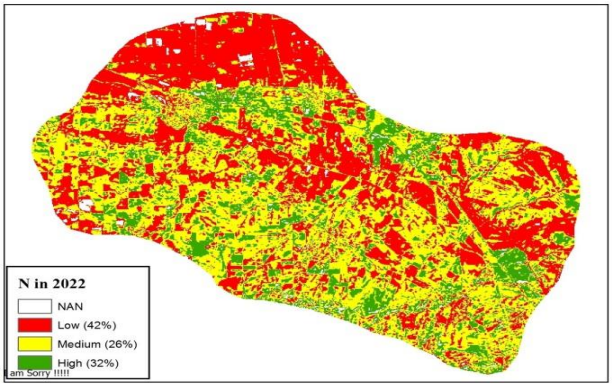

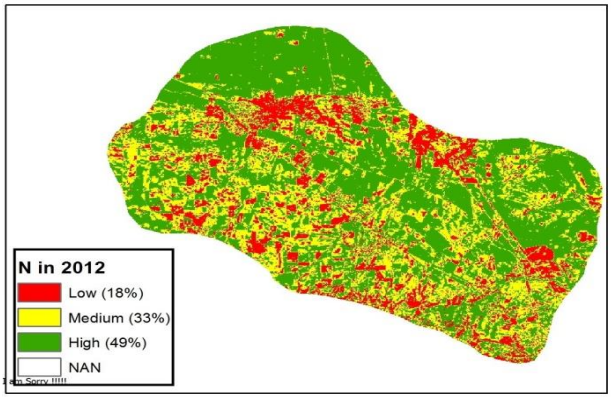

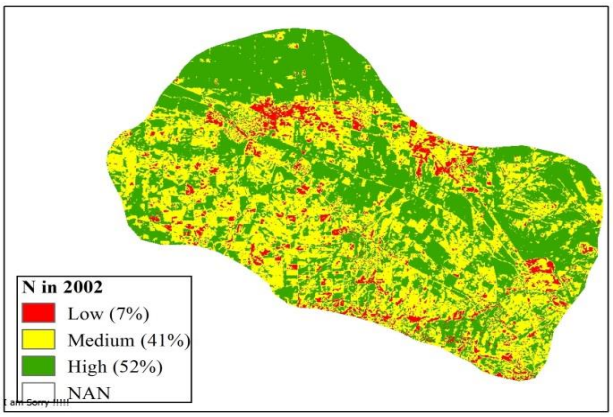

Figure 3: Maps of the distribution of areas of nitrogen varieties within the study area

The area of (High) decreased during the years 2002-2012 and 2012-2022 by 5% and 34%, respectively. As for the (Medium) variety, it decreased during the years 2002-2012 and 2012-2022 by 19% and 21%, respectively. This decrease in the area of the two varieties (High) and (Medium) was at the expense of the increase in the area of the (Low) variety, as it increased by (61% and 57%) during the years 2002-2012 and 2012-2022, respectively, and the maps show these stages of deterioration. Figure (3).

These results are attributed to several reasons, including that the studied area was heavily exploited by cultivating wheat, barley and some types of vegetables that depend on fertilization and supplying the land with its need of nitrogen fertilizer in 2002, in contrast to the percentage of the area exploited in 2012, as well as the clear difference in the amount of cultivated land in 2022. , where the cultivated area has clearly decreased, and the percentage of barren lands that are often poor in nitrogen, which suffer from loss conditions, has increased.

phosphorus:

Figure (4) shows the extent of the deterioration in the amount of ready phosphorous during the past twenty years. The predictive model (Equation 9) had a high accuracy in describing the state of phosphorous for the years 2022, 2012 and 2002, where the value of R2 of the predictive model for phosphorus was (0.9492). Kim and others (2014) mentioned that the adoption of predictive models obtained from remote sensing data contributes to the preparation of digital maps with high to acceptable accuracy to estimate the amount of ready phosphorus in the soil, in addition to the possibility of studying large areas within agricultural fields based on the same predictive model. Preparing spatial maps of the amount and distribution of phosphorous so that these maps will later be an important reference for researchers in soil fertility and surveys. There was a clear significant deterioration in the amount of ready phosphorous between the years 2002 and 2012 and the years 2012 and 2022, with a percentage of (8% and 100%) for the High variety, respectively, and for the Medium variety, the deterioration rate was (5% and 14%) for the years, respectively. . As for the Low variety, its area increased between 2002 and 2012 and 2012 and 2022 by (21% and 36%) for each, respectively. Figure (5).

The decline in the availability of ready-made phosphorous over time is natural. We often find this in poorly exploited agricultural fields and in limestone soils in particular. The high percentage of calcium carbonate content in the soil affects the readiness of most nutrients, including phosphorous. We will also mention later that there is a significant relationship between the increase in the soil content of calcium carbonate and the decrease in the availability of nutrients, as there was an increase in the area of limestone soils over time and this was accompanied by the deterioration of fertility characteristics. Ando et al. (2022) stated that the type of agricultural activity has a significant impact on the availability of phosphorus in the soil, and leaving the soil in a waste area has a clear effect on phosphorus fixation.

These results are in agreement with the findings of Al-Waeli (2019) in his study of phosphorous deterioration over time using predictive models obtained from remote sensing data, where there was a decrease in the availability of phosphorous between 1994 and 2014, and this was attributed to a decrease in the soil content of organic matter and a high temperature Soil interaction over time in arid and semi-arid areas as a result of mismanagement and many other factors.

Maddahi et al. (2015) emphasized the pedogenic and genetic importance of studying phosphorus in soil over time, as this represents a pedogenic function for the role of human activity in the development of soil resource through agricultural practices that activate the solubility of phosphate compounds in the soil. The ready-

made phosphorous maps represent an effective guiding method for raising farmers' awareness in dealing with phosphate fertilization, in a way that saves them high economic costs that can be used to manage other farm affairs.

These results are also in agreement with the findings of Bascietto et al. (2021) when they studied the fertility deterioration over time in wheat-growing areas in central Italy, where they found a significant relationship between predictive models and the status of laboratory measured phosphorus in soil. However, they recommended not to rely on the NDVI spectral index and its reflectivity values in evaluating major elements, including phosphorous, and to rely on other spectral indices that gave a relationship with the measured concentrations in the soil.

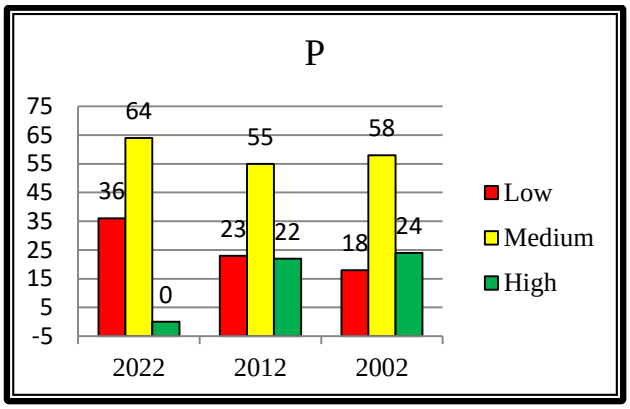

Figure (4): Percentages of the area of phosphorous value varieties in the years studied.

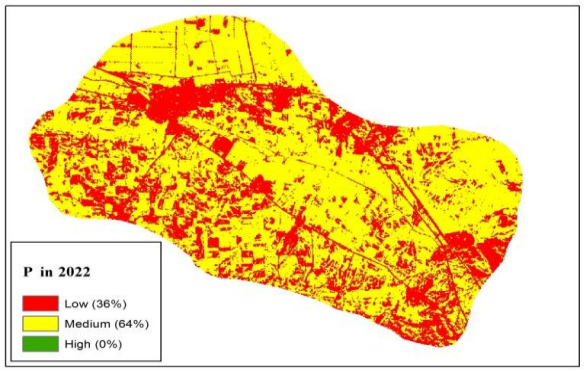

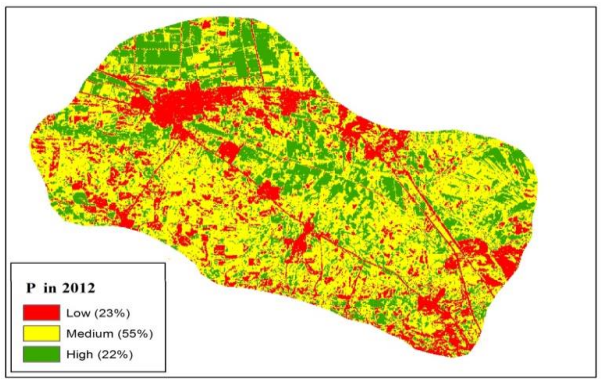

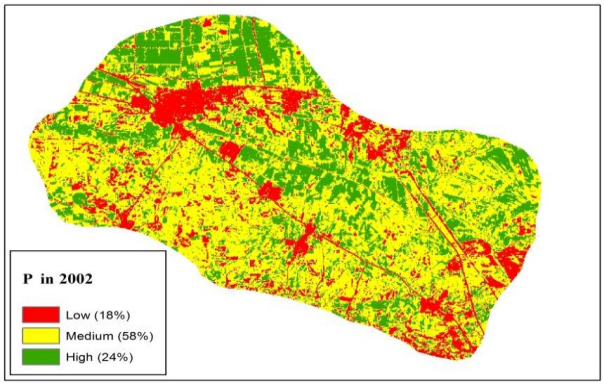

Figure (5): Maps of the distribution of areas of phosphorous varieties within the study area

Potassium

It appears from Figure (7) that the predictive model for potassium (Equation 10) (R2 = 0.6970) has given good results to describe the state of ready potassium for the years 2022, 2012 and 2002 within the three categories (High, Medium, Low), and the results of the maps and percentages showed. In Figure (6), there is a clear deterioration in the amount of ready potassium over time and a decline in the area of the two varieties High and Medium between the years 2002 and 2012, so the deterioration rate reached (45.7% and 6.4%) for the two types, respectively, while between the years 2012 and 2022, the rate of deterioration for the two types reached High and Medium (57.8% and 36.3%), respectively. As for the area of the Low category, it increased significantly between the years 2002 and 2012 and the years 2012 and 2022, the percentage of increase was (51.3% and 42.1%) for each of them, respectively.

The increase in the cation exchange capacity could be one of the reasons for the decrease in

the amount of potassium ready in the soil, as Al-Nuaimi (1999) mentioned that the soil with a high cation exchange capacity needs a larger amount of potassium to saturate it. Likewise, the type of agricultural activity and stressful agriculture that depends on the elements inherent in the soil (without fertilization) has a role in the decrease of the ready nutrients. In addition, it can be considered that the potassium installed during a period of time has a role in the development of future fertilizer plans.

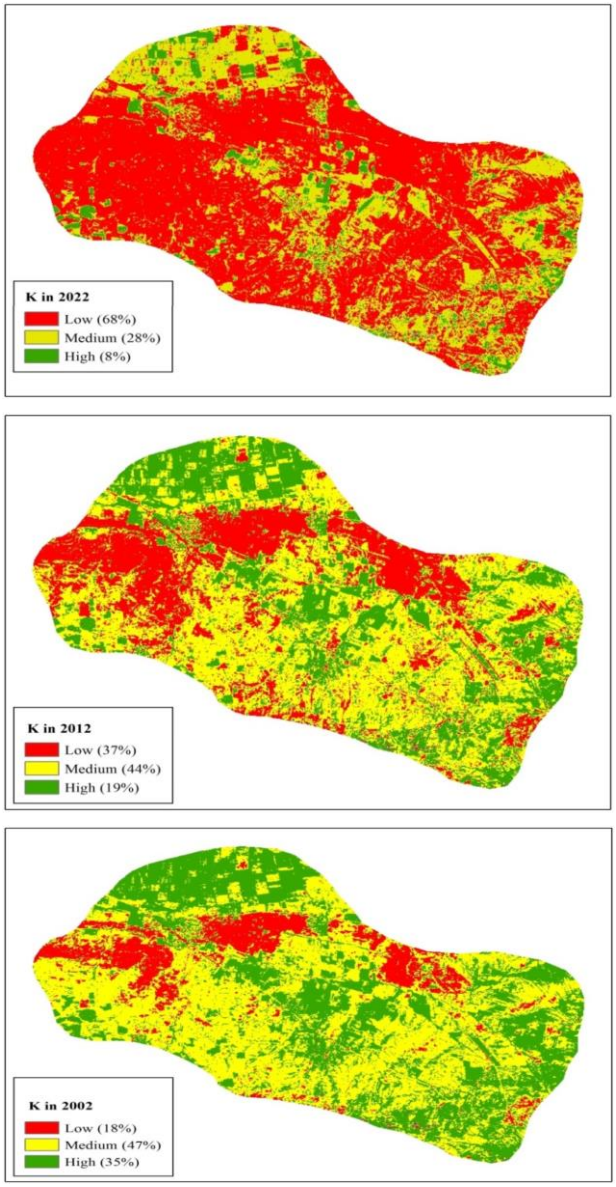

Figure (7): Area distribution maps of potassium varieties within the study area

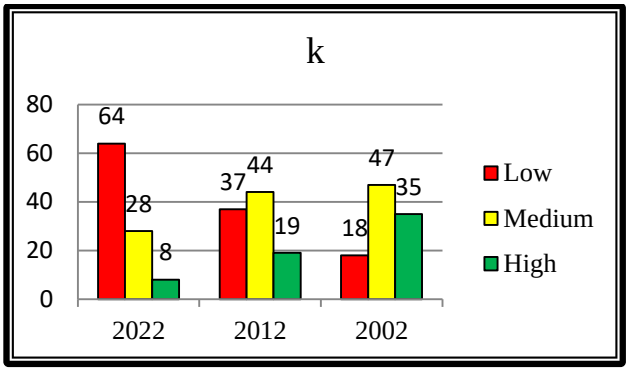

Figure (6): Percentages of the area of potassium values varieties in the years studied.

Goulding K. (2021) stated that potassium is one of the elements that is washable and seeps into the ground water over time, and due to its close connection with clay and organic matter and its presence in the surface layer, it is subject to loss during wind and water erosion processes, and he also mentioned that the operations of burning agricultural crops after harvesting lead to great loss With nutrients, including potassium. Lu et al. (2021), when using remote sensing data to estimate potassium in rice plants, showed that potassium becomes less ready for uptake by the plant as the soil moisture decreases. Last few years .

Conclusions

There is a strong relationship between the concentration of nutrients in the soil and the values of spectral indices and reflectivity indicators, and a strong relationship between the results of the predictive model and the values of the concentrations measured in the laboratory. It was also found that there was a clear deterioration in the availability of nutrients (N, P, K) during the time period between 2002 and 2022.

References

Abbas A., Khan S., (2007). Using remote sensing techniques for appraisal of irrigated soil salinity. In: Oxley, L. and Kulasiri, D., Eds., MODSIM 2007 International Congress on Modelling and Simulation, Modelling and Simulation Society of Australia and New Zealand, 2632-2638.

Adamu, G. K. , Yusuf, M. A. , and Ahmed M. , (2014). Soil Degradation in Dry Lands .

Academic Research International. Vol. 5 . No. 1. January. PP:78-91.

Al-Nuaimi, S. N. A., (1999). Fertilizer and soil fertility. Ibn Al-Atheer House for Printing and Publishing. University of Al Mosul. Nineveh. Iraq .

Ando, K., Yamaguchi, N., Kasuya, M., Oga, T., Ohashi, Y., and Taki, K. , (2022). Long-term (nearly a century) effects of fertilizer, lime and rice straw compost application on active aluminum and iron and available phosphorus in paddy fields. Geoderma, 424, 115992.

Bascietto, M., Santangelo, E., and Beni, C. , (2021). Spatial Variations of Vegetation Index from Remote Sensing Linked to Soil Colloidal Status. Land, 10(1), 80.

Gitelson, A., (2002). "Vegetation and Soil Lines in Visible Spectral Space: A Concept and Technique for Remote Estimation of Vegetation Fraction. International Journal of Remote Sensing 23: 2537–2562.

Goulding, K., (2021). Outputs: Potassium Losses from Agricultural Systems. In: Murrell, T.S., Mikkelsen, R.L., Sulewski, G., Norton, R., Thompson, M.L. (eds) Improving Potassium Recommendations for Agricultural Crops. Springer, Cham.

Huete, A. R.; Liu, H. Q.; Batchily, K.; Van Leeuwen, W. J. D., (1997). A comparison of vegetation indices over a global set of TM images for EOS-MODIS. Remote Sensing of Environment, Salt Lake City, v. 59, p. 440-451.

Kim, J., Grunwald, S., Osborne, T.Z., Robbins, R., Yamataki, H., Rivero, R.G., (2014). Spatial resolution effects of remote sensing images on digital soil models in aquatic ecosystems. In: Minasny, B., Malone, B.P., McBratney, A.B. (Eds.), Digital Soil Assessments and beyond. Taylor and Francis Group, London, pp. 121–125.

Maddahi , Z . , Jalallan A ., Zarkesh M . K . and Honarjo N ., (2015) . Providing a soil fertility map using geographic information system , Geostatistical techniques and fuzzy logic .Advances in Environmental Sciences International Journal of Bioflux Society .V.7 (1) : 131 – 138

Prudnikova, E. Y., Savin, I. Y., and Vindeker, G. V. (2021). Possibilities of remote sensing monitoring of soil fertility indicators of arable soils. In IOP Conference Series: Earth and Environmental Science (Vol. 862, No. 1, p. 012008). IOP Publishing.

Rondeaux, G., Steven M., and Baret. F., (1996). "Optimization of Soil-Adjusted Vegetation Indices." Remote Sensing of Environment 55: 95-107.

Rouse, J., Haas R., Schell J., and Deering D., (1973). Monitoring Vegetation Systems in the Great Plains with ERTS. Third ERTS Symposium, NASA: 309-317.

Storey, J., Choate, M., Lee, K., (2014). Landsat 8 operational land imager on-orbit geometric calibration and performance. Rem. Sens. 6, 11127–11152. https://doi.org/10.3390/rs61111127

Taha, A. M., and Ihab K. E., (2014). Diagnosis of salt degradation from the chemical properties of sodic and non-sodic soils and remote sensing data. Al-Qadisiyah Journal of Agricultural Sciences. 2(4): 67-81.

Vagan , Tor-G . , L . Winowiecki , J . E . Tondoh , L . T . Desta and T . Gumbricht . , (2016). Mapping of soil properties and land degradation risk in Africa using MODIS reflectance . Geoderma . 263 : 216 – 225 .

Wu , W . , (2011) . Atmospheric Correction for Landsat Data – Mterial for remote sensing training . ICARDA .w.wu@cgiar.org

Wu, W. , (2014). The Generalized Difference Vegetation Index (GDVI) for Dry land Characterization. Remote Sens. 6: 1211-1233.